ACS OMEGA

Open Access



http://pubs.acs.org/journal/acsodf

Article

# Citropten Inhibits Vascular Smooth Muscle Cell Proliferation and Migration via the TRPV1 Receptor

Thi Hoa Pham,[‡] Nguyen Minh Trang,[‡] Eun-Nam Kim, Hye Gwang Jeong, and Gil-Saeng Jeong*

Cite This: *ACS Omega* 2024, 9, 29829−29839

Read Online

ACCESS | Metrics & More | Article Recommendations | Supporting Information

**ABSTRACT:** Vascular smooth muscle cell (VSMC) proliferation and migration play critical roles in arterial remodeling. Citropten, a natural organic compound belonging to coumarin and its derivative classes, exhibits various biological activities. However, mechanisms by which citropten protects against vascular remodeling remain unknown. Therefore, in this study, we investigated the inhibitory effects of citropten on VSMC proliferation and migration under high-glucose (HG) stimulation. Citropten abolished the proliferation and migration of rat vascular smooth muscle cells (RVSMCs) in a concentration-dependent manner. Also, citropten inhibited the expression of proliferation-related proteins, including proliferating cell nuclear antigen (PCNA), cyclin E1, cyclin D1, and migration-related markers such as matrix metalloproteinase (MMP), MMP2 and MMP9, in a concentration-dependent manner. In addition, citropten inhibited the phosphorylation of ERK and AKT, as well as hypoxia-inducible factor-1$\alpha$ (HIF-1$\alpha$) expression, mediated to the Krüppel-like factor 4 (KLF4) transcription factor. Using pharmacological inhibitors of ERK, AKT, and HIF-1$\alpha$ also strongly blocked the expression of MMP9, PCNA, and cyclin D1, as well as migration and the proliferation rate. Finally, molecular docking suggested that citropten docked onto the binding site of transient receptor potential vanilloid 1 (TRPV1), like epigallocatechin gallate (EGCG), a well-known agonist of TRPV1. These data suggest that citropten inhibits VSMC proliferation and migration by activating the TRPV1 channel.

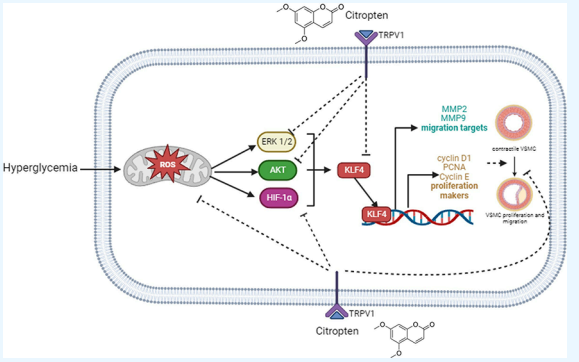


## 1. INTRODUCTION

Cardiovascular diseases and conditions, including myocardial infarction, atherosclerosis, stroke, ischemic heart disease, hyperplasia, and hypertension, are the leading causes of death worldwide.[1,2] Vascular smooth muscle cells (VSMCs) are prominent components of the vascular wall that play a crucial role in maintaining vascular homeostasis. Abnormal proliferation and migration of VSMCs following vascular injury are critical events for developing atherosclerosis and intimal hyperplasia.[3,4] Physiologically, VSMCs exist in a quiescent contractile state to regulate the vascular tone via vessel constriction.[5] However, in response to vascular injury, stress conditions, and various stimuli, including hypoxia, reactive species, and growth factors, VSMCs dedifferentiate into a proliferative, synthetic, and migratory phenotype.[6−8]

Phenotypic switching of VSMCs is commonly observed in atherosclerosis, intimal hyperplasia, hypertension, and post-angioplasty restenosis.[9,10] Elucidation of the mechanisms of VSMCs phenotypic switching may provide novel therapeutic targets for the prevention and treatment of these diseases. Aberrant VSMCs proliferation and migration play essential roles in the development of vascular diseases and conditions, such as atherosclerosis, restenosis, and hypertension.[11,12] Therefore, development of new strategies against VSMCs phenotypic switching, proliferation, and migration may aid the treatment of VSMC-related pathological conditions.

Transient receptor potential vanilloid type 1 (TRPV1) is a ligand-gated cationic channel with considerable $Ca^{2+}$ permeability. TRPV1 is expressed in blood vessels in the skeletal muscle, mesenteric and skin tissues, aorta, and carotid arteries.[13] TRPV1 is activated by many physical and chemical stimuli, including noxious heat, acidic pH, inflammatory mediators, and vanilloid compounds.[14] In addition to its key role in neuronal functions, TRPV1 also regulates the vascular tone, blood pressure, and pathogenesis of cardiovascular diseases.[15,16] Tissue-specific activation of TRPV1 channels stimulates the activation of the endothelial nitric oxide synthase (eNOS)−nitric oxide (NO) pathway in vascular endothelial cells, thus providing protection against cardiovascular diseases by regulating endothelium-dependent vasodilation and promoting angiogenesis. Moreover, TRPV1 is

Received: April 12, 2024
Revised: June 5, 2024
Accepted: June 7, 2024
Published: June 25, 2024

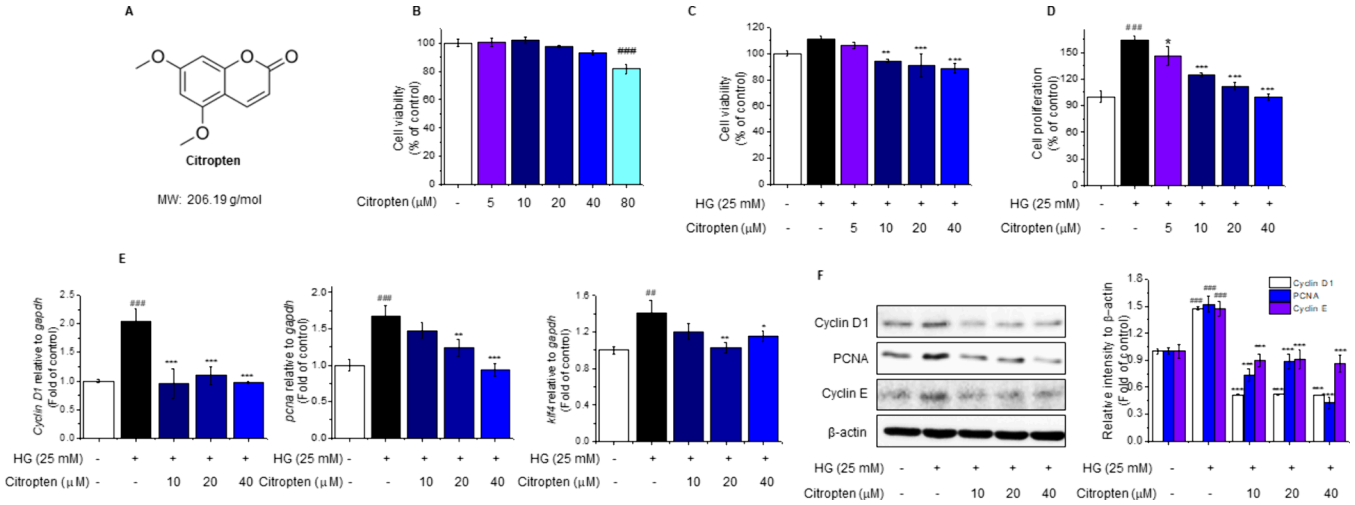


**Figure 1.** Citropten inhibited HG-induced RVSMCs proliferation. (A) Structure of citropten. (B, C) Cell cytotoxicity was evaluated by MTT assay. (D) Cell proliferation was examined by CCK-8 assay. (E) Realtime-PCR were conducted to detect mRNA expression of proliferation makers. (F) Western blot analysis was used to analyze protein levels in whole RVSMCs. Data are expressed as the mean ± SD. All experiments were performed in triplicate. $^{\#\#}p < 0.01$ and $^{\#\#\#}p < 0.001$ compared with control; $^{*}p < 0.05$, $^{**}p < 0.01$, and $^{***}p < 0.001$ compared with HG incubation.

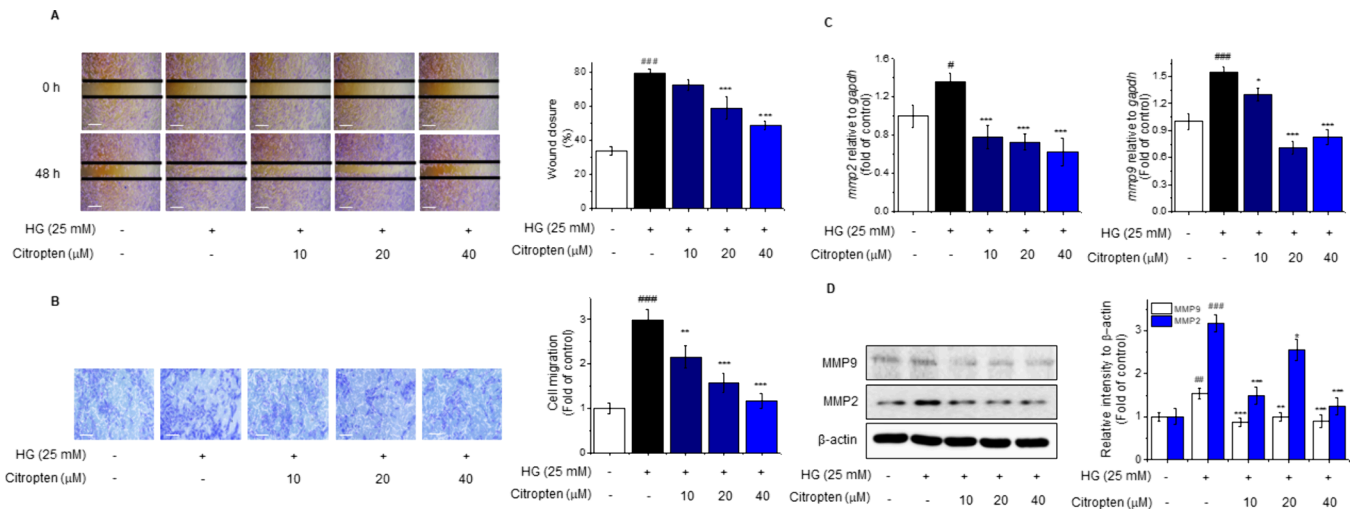


**Figure 2.** Citropten reduced HG-induced RVSMCs migration. RVMSCs were pretreatment with citropten for 1 h, followed with HG treatment for 48 h. (A) Wound-healing assay, the black lines indicate a clear zone after scratching (0 h). (B) Cell migration was evaluated by a trans-well migration assay. Scale bar = 100 μm. (C) PCR results were used to determine the expression of *mmp*2 and *mmp*9 mRNA. (D) Western blot analysis was used to detect protein levels in whole RVSMCs. Data are expressed as the mean ± SD. All experiments were performed in triplicate. $^{\#}p < 0.05$ and $^{\#\#\#}p < 0.001$ compared with control; $^{*}p < 0.05$, $^{**}p < 0.01$, and $^{***}p < 0.001$ compared with HG treatment.

abundantly expressed in VSMCs and activation TRPV1 by capsaicin leads to arteriole constriction.[17] Overexpression of TRPV1 closely involved in inhibiting VSMC migration and phenotype transitions-induced by angiotensin II (Ang II).[18] Activation of TRPV1 blocked VSMC proliferation and migration by upregulating the expression of peroxisome proliferator-activated receptor alpha (PPARα).[19]

Citropten (5,7-dimethoxycoumarin, limettin) is a coumarin derivative that exhibits various biological activities. It exerts antiproliferative effects on B16 melanoma cells[20] and preventive effects against chronic-depression-induced mild stress in rats.[21] Recently, we demonstrated that citropten ameliorates osteoclastogenesis related to the mitogen-activated protein kinase (MAPK) and phospholipase Cγ (PLCγ)/$Ca^{2+}$ signaling pathway.[22] However, to date, no studies have investigated the effects of citropten on the proliferation and migration of VSMCs and the association between citropten and the TRPV1 channel. Therefore, we aimed to explore the roles and mechanisms of action of citropten in the regulation of the VSMC physiology.

## 2. RESULTS

**2.1. Citropten Inhibits High Glucose (HG)-Induced RVSMCs Proliferation.** To assess the effect of citropten on RVSMCs proliferation, we examined the cytotoxicity effects of citropten on RVSMCs using the 3-[4,5-dimethylthiazol-2-yl]-2,5-diphenyl tetrazolium bromide (MTT) assay. As depicted in Figure 1B, citropten (5, 10, 20, and 40 μM) did not exert any cytotoxic effects on RVSMCs. Therefore, these concentrations were selected for subsequent experiments. HG was used to induce cell proliferation, as described previously.[23] Here, HG enhanced the cell viability and proliferation. HG-stimulated increase in cell proliferation was gradually inhibited via pretreatment with citropten in a concentration- dependent


https://doi.org/10.1021/acsomega.4c03539
ACS Omega 2024, 9, 29829−29839

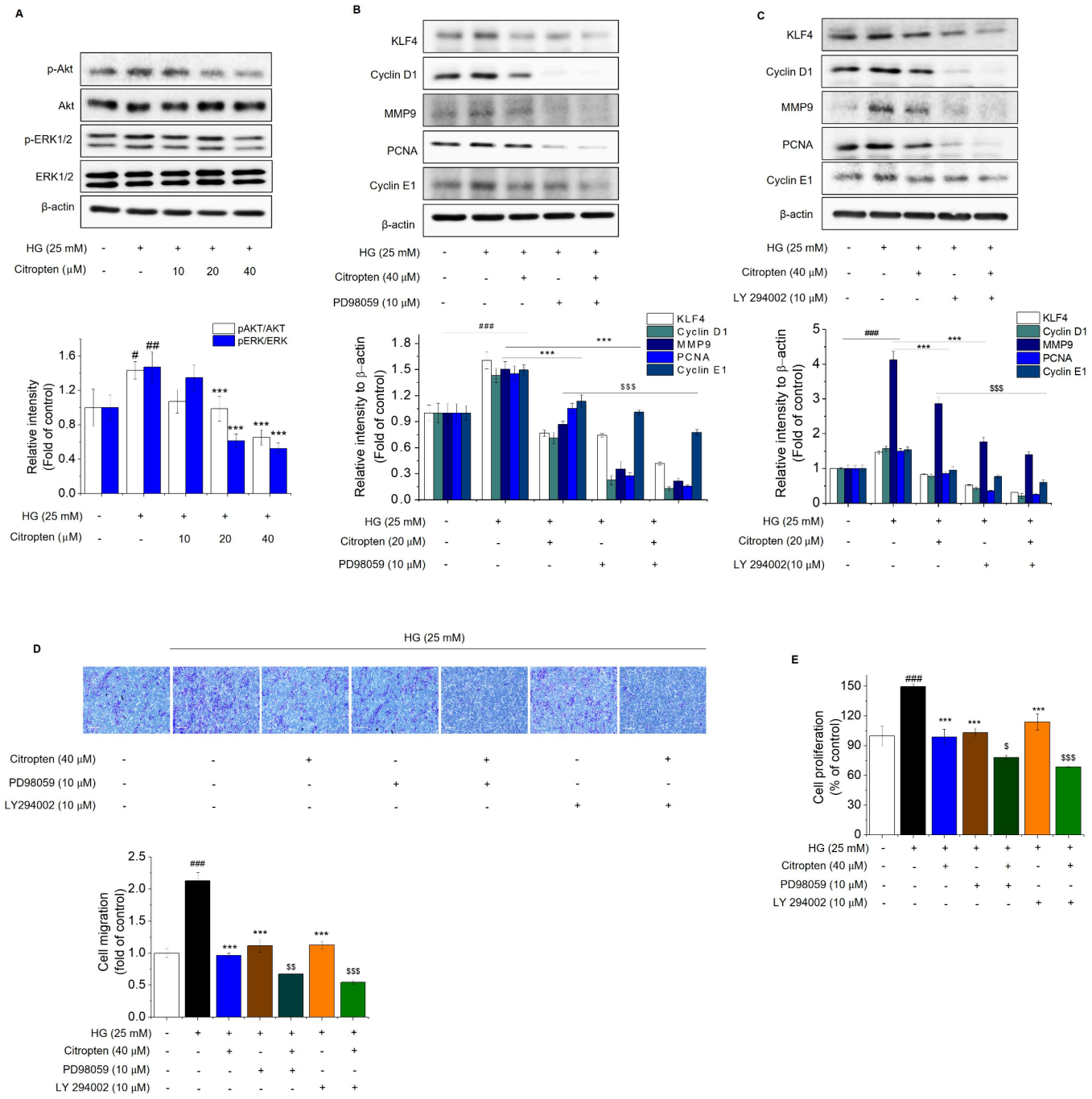


**Figure 3.** Citropten prevented HG-induced migration and proliferation in RVSMCs related ERK and AKT signaling pathway. (A) RVSMCs were pretreated with citropten for 1 h before being incubated with HG for 30 min. (B−E) RVSMCs were preincubated with LY294002 or PD98059 and/or citropten for 1 h and then exposed to HG for 24−48 h. (B, C) Western blot analysis was used to analyze the levels of the indicated proteins in-cell lysates. (D) Migration effect was assessed by trans-well assay. Scale bar = 100 $\mu$m. (E) CCK-8 assay was conducted to evaluate cell proliferation. Results are represented as means ± SD ($n$ = 3), $^{\#}p < 0.05$, $^{\#\#}p < 0.01$, and $^{\#\#\#}p < 0.001$ compared with control; $^{***}p < 0.001$ compared with HG treatment; $^{\$}p < 0.05$, $^{\$\$}p < 0.01$, and $^{\$\$\$}p < 0.001$ compared with citropten plus HG treatment.

manner. The results of the cell counting kit-8 assay were similar to those of the MTT assays, indicating that citropten reduces the proliferation of RVSMCs (Figure 1C,D). Consistently, HG increased the mRNA and protein levels of cyclin D1, KLF4, proliferating cell nuclear antigen (PCNA), and other proliferation markers. However, pretreatment with citropten reversed these effects (Figure 1E,F). Decreased contractile marker levels, increased synthetic marker levels, and increased proliferation rate are the main features of VSMCs phenotypic switching.[4] As indicated in Figure S1, the effect of citropten on the HG-induced shift toward the synthetic phenotype was revealed by immunofluorescence and Western blotting of the contractile marker, SM22. HG downregulated SM22, but pretreatment with citropten recovered its expression. These results suggest that citropten prevents HG-induced phenotypic switching and proliferation of VSMCs.

**2.2. Effect of Citropten on HG-Induced RVSMCs Migration.** Wound healing and transwell assays were



https://doi.org/10.1021/acsomega.4c03539
ACS Omega 2024, 9, 29829−29839

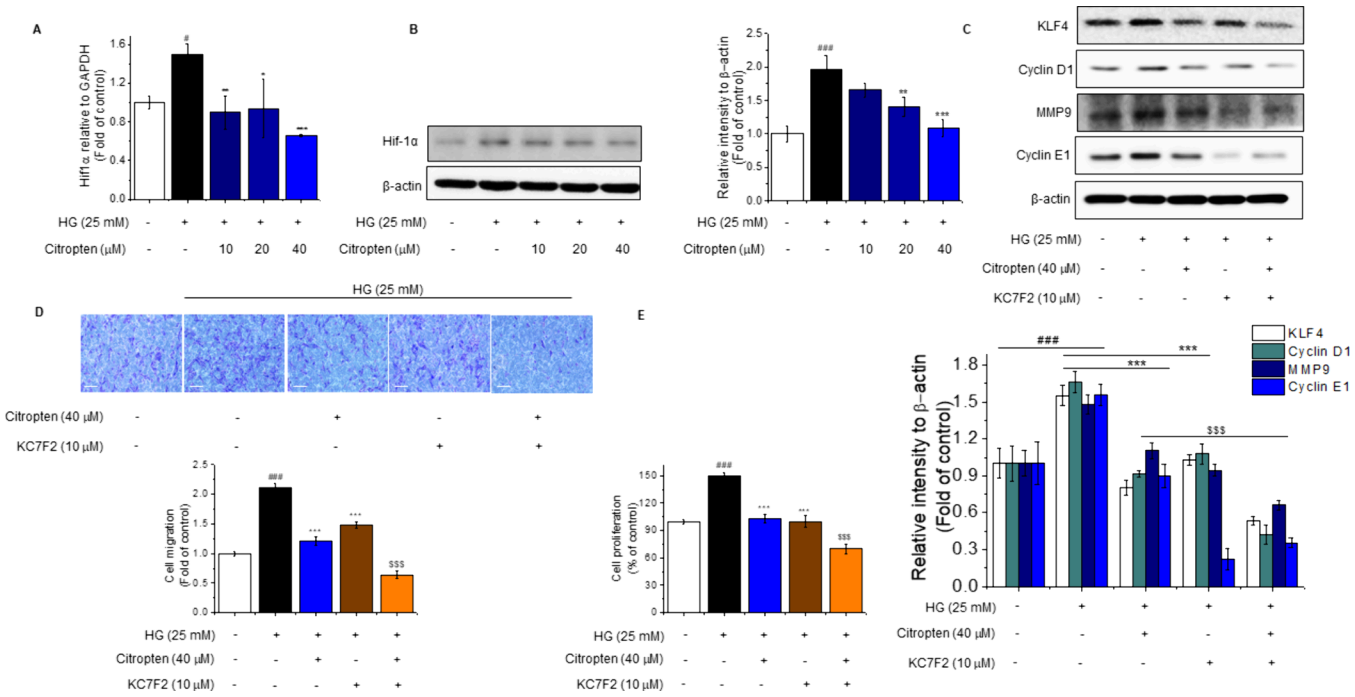


**Figure 4.** Citropten prevented HG-induced migration and proliferation in RVSMCs related to the HIF-1$\alpha$ pathway. (A, B) RVSMCs were pretreated with citropten for 1 h before being incubated with HG for 24 h. Results was assessed by PCR (A) and Western blot assay (B). (C−E) RVSMCs were preincubated with KC7F2 and/or citropten for 1 h, and then exposed to HG for 24−48 h. (C) Western blot analysis was used to analyze the levels of the indicated proteins in-cell lysates. (D) Migration effect was performed by trans-well assay. Scale bar = 100 $\mu$m. (E) Cell proliferation was obtained from CCK-8 assay. Results are represented as means ± SD ($n$ = 3), $^{\#}p < 0.05$ and $^{\#\#\#}p < 0.001$ compared with control; $^{*}p < 0.05$, $^{**}p < 0.01$, and $^{***}p < 0.001$ compared with HG treatment, $^{\$\$\$}p < 0.001$ compared with citropten plus HG treatment.

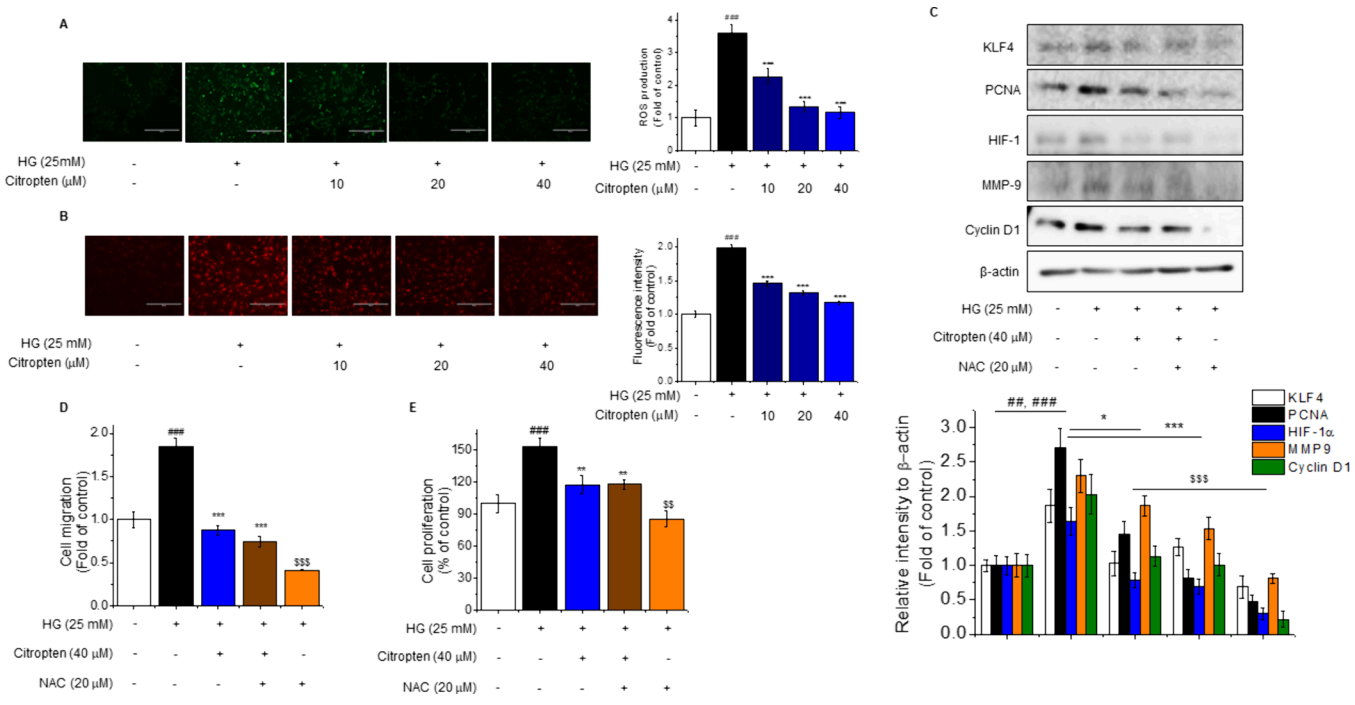


**Figure 5.** Citropten prevented HG-induced ROS production in RVSMCs. (A, B) RVSMCs were pretreated with citropten for 1 h and then stimulated with HG for an additional 24 h. The intracellular superoxide levels were measured by DCFHDA assay (A). Mitochondrial superoxide generation was examined using MitoSOX staining (B). Scale bar = 200 $\mu$m. (C−E) RVSMCs were pretreated with citropten in the presence or absence of NAC for 1 h, before 24−48 h of exposure to HG. (C) Western blot was used to analyze the levels of proteins in cells. (D) Migration effect was assessed by trans-well assay. (E) CCK-8 assay was conducted to evaluate cell proliferation. Results are presented as means ± SD ($n$ = 3). $^{\#\#}p < 0.01$ and $^{\#\#\#}p < 0.001$ compared with control; $^{*}p < 0.05$, $^{**}p < 0.01$, and $^{***}p < 0.001$ compared with HG treatment; $^{\$\$}p < 0.01$ and $^{\$\$\$}p < 0.001$ compared with citropten plus HG treatment.



https://doi.org/10.1021/acsomega.4c03539
ACS Omega 2024, 9, 29829−29839

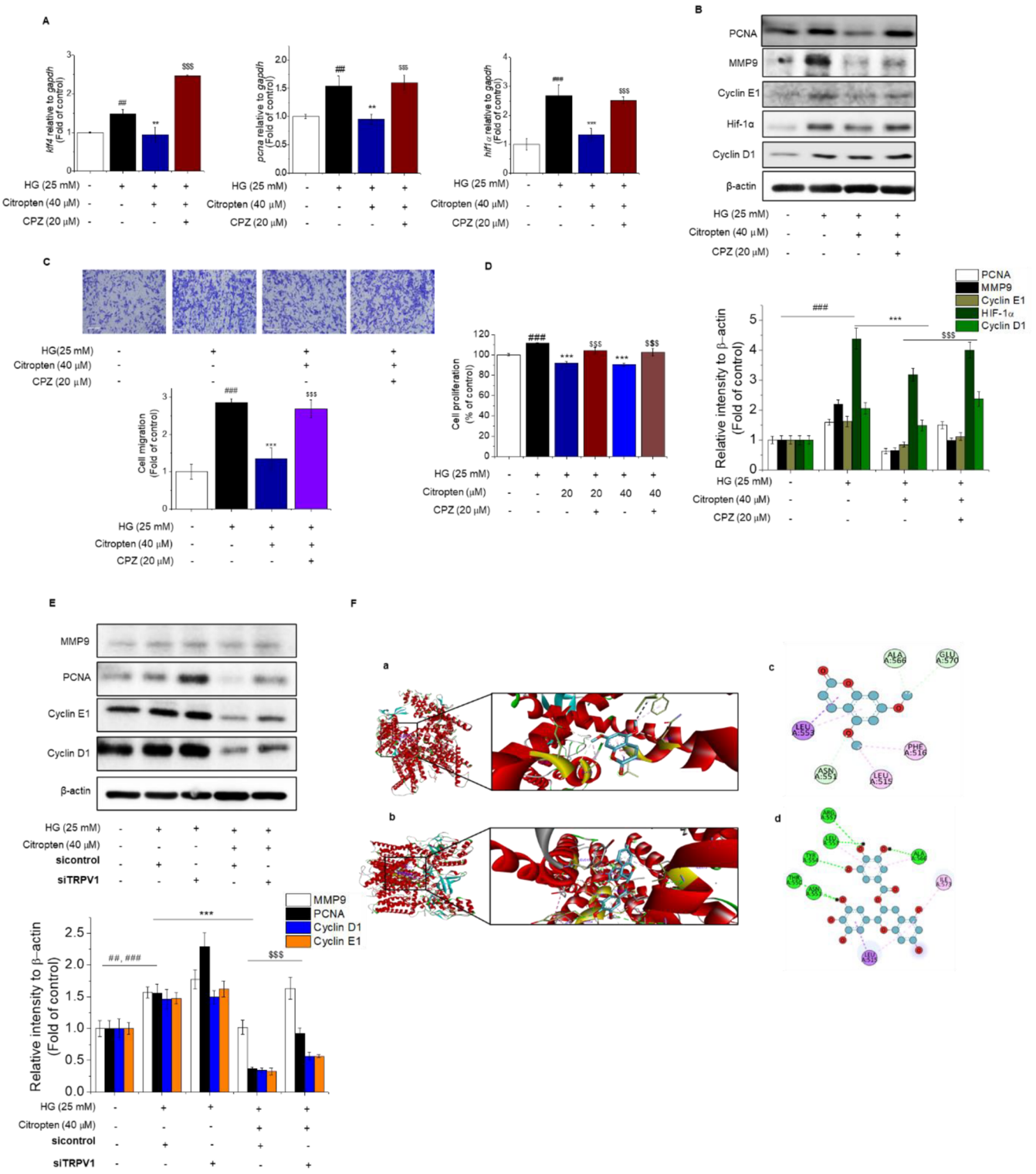


**Figure 6.** Citropten inhibited RVSMCs proliferation and migration through TRPV1 channel. (A–D) RVSMCs were pretreated with citropten in the presence or absence of CPZ for 1 h, before 24–48 h of exposure to HG. (A) Results were assessed by PCR. (B) Western blot was used to analyze the levels of indicated proteins in the whole-cell lysates. (C) Migration rate was assessed by a trans-well assay. Scale bar = 100 $\mu$m. (D) CCK-8 assay was conducted to determine cell proliferation rate. (E) RVSMCs cells were transfected with a siRNA TRPV1 for 24 h, followed by incubation with citropten in the absence or presence of HG for 24 h. The results were evaluated by Western blot. (F) Proposed docking model of TRPV1 homology model in 3D in 2D with Citropten (a, c) and EGCG (b, d). $^{\#\#}p < 0.01$ and $^{\#\#\#}p < 0.001$ compared with control; $^{***}p < 0.001$ compared with HG treatment with or without siRNA control transfection; $^{\$\$\$}p < 0.001$ compared with citropten plus HG treatment with or without siRNA control transfection. All experiments were performed in triplicate.



https://doi.org/10.1021/acsomega.4c03539
ACS Omega 2024, 9, 29829–29839

performed to determine the effect of citropten on RVSMCs migration. Migration rates were recorded at 0 and 48 h. As shown in Figure 2A,B, HG promoted wound closure and cell migration compared with those in the untreated cells (Figures 2A and B) after 48 h. However, pretreatment with citropten reversed these effects. Consistently, the levels of migration-related markers, such as matrix metalloproteinase (MMP)-2 and MMP9, increased in response to HG stimulation, but pretreatment with citropten completely reversed these effects (Figure 2C,D).

**2.3. Citropten Inhibits HG-Activated AKT and Extracellular Signal-Regulated Kinase (ERK) Pathway in RVSMCs.** ERK and AKT pathways are closely associated with VSMC proliferation and migration.[24,25] Therefore, the effects of citropten on the ERK and AKT pathways were investigated in this study. As depicted in Figure 3A, pretreatment with citropten abolished HG-enhanced AKT and ERK phosphorylation in a concentration-dependent manner (Figure 3A). Pharmacological inhibitors of AKT (LY294002) and ERK (PD98059) completely blocked HG-induced cell migration and proliferation (Figure 3B,C). Interestingly, these inhibitors enhanced the inhibitory effects of citropten under cotreatment conditions. Similar results were observed in the proliferation and migration assays (Figure 3D,E). Thus, these data indicate that citropten inhibits HG-induced cell migration and proliferation by inhibiting the AKT and ERK pathways.

**2.4. Citropten Blocks the HG-Activated HIF-1$\alpha$ Signaling Pathway in RVSMCs.** HIF-1$\alpha$ is potentially associated with the phenotypic switching of VSMCs. HIF-1$\alpha$ is a transcriptional regulator that binds to the regulatory sites of promoters to promote the production of VSMC proliferation-related growth factors.[26−28] To examine whether citropten inhibits the migration and proliferation of RVSMCs and the HIF-1$\alpha$ pathway, we investigated the expression of HIF-1$\alpha$ under conditions of citropten treatment in the absence or presence of HG. As shown in Figure 4A,B, HG strongly increased HIF-1$\alpha$ expression at the transcript and protein levels. Pretreatment with citropten significantly blocked HIF-1$\alpha$ expression (Figure 4C). Moreover, a pharmacological inhibitor of HIF-1$\alpha$ (KC7F2) not only downregulated the expression of proliferation and migration markers but also enhanced the inhibitory effects of citropten on these targets. These results suggest that citropten ameliorates the HG-induced increase in the migration and proliferation of VSMCs mediated by the HIF-1$\alpha$ signaling pathway.

**2.5. Citropten Prevents HG-Induced ROS Production in RVSMCs.** Excess ROS bioactivity is a key mechanism underlying phenotype switching of VSMC.[10] Therefore, we investigated the effect of citropten on the vascular ROS viability in this study. As shown in Figure 5A, HG significantly increased the ROS production in RVSMCs; however, citropten markedly inhibited this effect (Figure 5A). Similarly, citropten inhibited HG-induced mitochondrial ROS production (Figure 5B). To validate the role of ROS, cells were pretreated with NAC (N-acetyl-L-cysteine) (an ROS inhibitor) for 1 h and citropten for 3 h, followed by incubation in the absence or presence of HG for 24−48 h. NAC strongly blocked the expression of MMP9, cyclin D1, PCNA, KLF4, and HIF-1$\alpha$ induced by HG. Moreover, the inhibitory effects of the citropten and NAC combination were stronger than those of either compound alone (Figure 5C). Similar results were obtained in the proliferation and migration assays (Figure 5D,E). Therefore, citropten inhibits the proliferation and migration of RVSMCs by suppressing the ROS production.

**2.6. Citropten Inhibits RVSMCs Proliferation and Migration via the TRPV1 Channel.** TRPV1 is closely associated with vascular function.[13,17−19] To explore whether TRPV1 is involved in the citropten-mediated alteration of RVSMCs physiological functions, we used a selective antagonist of TRPV1, capsazepine (CPZ). Pretreatment with CPZ reversed the effects of citropten on migration and proliferation markers at the transcript and protein levels (Figure 6A,B). Cell proliferation and migration assays showed similar results (Figure 6C,D). To confirm these observations, cells were transfected with a small interfering RNA against TRPV1. Consistently, TRPV1 knockdown did not affect the HG-stimulation-induced cell migration and proliferation (Figure 6E). Docking studies of epigallocatechin gallate (EGCG, a well-known agonist of TRPV1)[29] and citropten were performed based on a homology model of TRPV1. As shown in Figure 6F, crystal structures of citropten and EGCG showed hydrogen bond interactions with Ala566 and Asn551. Additionally, the flavonoid scaffold of citropten revealed hydrophobic interactions with the side chain of Leu515 in TRPV1 with a docking model similar to that of EGCG (Figure 6F). Binding affinity and root-mean-square deviation (RMSD) between citropten and the identical virtual structure were −6.3 and 1.422 Å, respectively, whereas those between EGCG and TRPV1 were −8.0 and 0.009 Å, respectively. Analysis of docking models of TRPV1 and citropten suggested that citropten acts as a TRPV1 agonist. Taken together, our data suggest that citropten inhibits the HG-induced proliferation and migration of RVSMCs via the TRPV1 channel.

## 3. DISCUSSION

Diabetes is a primary risk factor for atherosclerosis, stroke, coronary heart disease, and dyslipidemia. Increased risk and accelerated development of atherosclerosis have been reported in patients with diabetes and high blood pressure.[30] In this study, we demonstrated a novel role of citropten in regulating VSMCs proliferation and migration in response to HG. The mRNA and protein expression of proliferation markers (cyclin D1, cyclin E1, and PCNA) and migration targets (MMP2 and MMP9) was inhibited by citropten in HG-challenged cultured RVSMCs. Citropten greatly decreased RVSMCs proliferation and migration rate, and the ROS production induced by HG mediated the AKT, ERK, and HIF-1$\alpha$ signaling pathway. The effect of citropten was partly dependent on TRPV1 receptor activation.

Abnormal proliferation and migration of RVSMCs play crucial roles in the development of atherosclerotic lesions. Among the multiple factors that drive the development of atherosclerosis, hyperglycemia is a major causative factor. Coutinho et al. reported that the risk of cardiovascular events starts at concentrations below the nondiabetic glucose range (<6.1 mM, and continues to act within the diabetic glucose range (>11.1 mM) in an exponential fashion.[31] HG triggered structural and functional changes in VSMCs involved in diabetic atherosclerosis by regulating several signaling pathways, including the generation of advanced glycation end products and oxidative stress.[32] In addition, HG activated the expression of genes participating in ERK-dependent mitogenic response and enhanced mitochondrial dysfunction, endoplasmic reticulum stress, and ROS accumulation in VSMCs. All of these factors stimulate the proliferation and migration of


https://doi.org/10.1021/acsomega.4c03539
ACS Omega 2024, 9, 29829−29839

VSMCs. Therefore, we chose HG as the *in vitro* stimulant. Citropten (10−40 $\mu$M) significantly inhibited the proliferation and migration of RVSMCs induced by HG (25 mM). Pretreatment with citropten reduced the expression of cyclin D1 and PCNA, which are proliferation markers. We designed a wound healing test and transwell cell migration assay to examine the migration ability of RVSMCs in response to HG stimulation. Citropten inhibited wound closure and cell migration, which was consistent with the expression of MMP2 and MMP9 at the mRNA and protein levels induced by HG in RVSMCs. Citropten also increased the protein levels of SM22, a specific contractile marker of RVSMCs. Our findings are consistent with previous studies that investigated the inhibitory effects of natural compounds such as luteolin, resveratrol, and EGCG on the migration and proliferation of RVSMCs.[33−35]

MAPK/ERK pathway is reported to be closely related to cell proliferation, differentiation, migration, senescence and apoptosis.[24] The PI3K/AKT signaling pathway is involved in various cellular processes, such as glucose metabolism, apoptosis, proliferation, and migration.[36] In this study, we observed that citropten also reduced the levels of phosphorylation of AKT and ERK in a concentration-dependent manner. These results align with those of our previous study on the effect of citropten on osteoclastogenesis inhibition in RAW264.7 cells.[22] Moreover, inhibition of AKT and ERK activity by pharmacological inhibitors not only inhibited the HG-induced cell migration and proliferation but also enhanced the inhibitory effects of citropten on HG-induced expression of related molecules, including MMP2, MMP9, PCNA, cyclin D1, cyclin E1, and KLF4. These results indicate that citropten inhibits HG migration and proliferation and plays a role in the inhibition of the AKT and ERK pathways.

HIF-1$\alpha$ is an important determinant of healing outcomes. It contributes to all stages of wound healing via cell division, growth factor release, and matrix synthesis.[37] HIF-1$\alpha$ was reported to promote the proliferation and migration of pulmonary arterial SMC via activation of Cx43.[26] The knockdown of HIF-1$\alpha$ inhibits the proliferation and migration of outer root sheath cells.[27] In addition, HIF-1$\alpha$ expression is upregulated by HG stimulation, indicating HIF-1$\alpha$ may widely define a novel strategic milieu for the intervention cardiac complications in patient with diabetes.[38] Therefore, we examined the role of HIF-1$\alpha$ in citropten-abolished HG-induced migration and proliferation. In this study, citropten blocked HIF-1$\alpha$ expression in a concentration-dependent manner. KC7F2 (a selective inhibitor of HIF-1$\alpha$) strongly prevented RVSMCs proliferation and migration. Importantly, cotreatment with KC7F2 and citropten showed greater inhibitory effects than KC7F2 or citropten treatment alone. Therefore, downregulation of HIF-1$\alpha$ is associated with antimigration and proliferation of citropten.

Excessive ROS accumulation causes vascular cell damage, activation of metalloproteinases, and deposition of extracellular matrix, collectively leading to vascular remodeling.[39] Therefore, we investigated the effect of citropten on ROS production in whole cells and mitochondria and the relationship between this inhibitory effect and cell migration and proliferation. Incubation with citropten significantly decreased the HG-induced increase in the intracellular and mitochondrial ROS production. Moreover, ROS inhibition by NAC not only suppressed HG-induced cell migration and proliferation rate and expression of related proteins but also enhanced the effect of citropten on the inhibition of these proteins. As mentioned in a previous study, citropten reduced ROS production.[22] Like several antioxidants, citropten exhibited potential and diverse effects for the prevention and treatment of cardiovascular diseases.

TRPV1 is a nonselective cation channel with a preference for calcium transmission.[17] The TRPV1 channel is involved in the regulation of calcium signaling, which is crucial for many cellular processes, including proliferation, apoptosis, secretion of cytokines, and T cell activation.[40] The activation of TRPV1 can reduce blood pressure and improve vascular damage.[41] Research on type 2 diabetes mellitus has confirmed that activation by capsaicin can improve glucose homeostasis, ameliorate hyperglycemia-induced endothelial dysfunction, and prevent diabetic cardiovascular complications. Hao et al. found that TRPV1 activation through chronic dietary capsaicin, reduced vascular dysfunction by preventing the generation of oxidative stress in mice with high salt intake-induced hypertension.[42] In the present study, citropten was considered a novel agonist of TRPV1 like EGCG, a well-known agonist of TRPV1, which is indicated by molecular docking results. Both, EGCG and citropten, formed hydrogen bonds with TRPV1 at Ala566 and Asn551, and were hydrophobic at Leu515. In addition, our data demonstrated that citropten exhibited a considerable ability to inhibit the HG-induced proliferation and migration of RVSMCs mediated by TRPV1 channels using pharmacological antagonists as well as silencing RNA against TRPV1, which reversed the inhibitory effect of citropten. Our results are consistent with previous data, demonstrating that TRPV1 activation inhibits phenotypic switching, oxidative stress, migration, and proliferation of RVSMCs.

In conclusion, this study revealed that citropten inhibited the HG-enhanced migration and proliferation of RVSMCs at the transcript and protein levels. Additionally, it inhibited cell proliferation and migration. Pretreatment with citropten reduced the ROS production in RVSMCs. The effects of citropten were mediated via the AKT, ERK, and HIF-1$\alpha$ signaling pathways, with KLF4 as the main transcription factor. Moreover, the protective effects of citropten were mediated via the TRPV1 channel. Considering the increasing incidence of diabetes and vascular diseases worldwide, which pose a serious threat to public health problems, the application of citropten may be beneficial for the prevention and treatment of diabetes-associated cardiovascular complications.

## 4. MATERIALS AND METHODS

**4.1. Plant Materials.** The citropten used in this study was isolated from the peels of *C. aurantifolia*. The peels of *C. aurantifolia* were purchased at a local market within the Daegu Herbal Medicine Market in 2020. Voucher specimens of *C. aurantifolia* peels (CNU-NPLP-062) were maintained in the Natural Products Laboratory, College of Pharmacy, Chungnam National University. The isolation method and NMR spectroscopy of citropten were described in a previously reported literature (Menezes et al., 2014).[22]

**4.2. Materials.** MTT (3-(4,5-dimethylthiazol-2-yl)-2,5-diphenyltetrazolium bromide, cat. no. M2128) and DCFHDA (cat. no. 35845) were sourced from Sigma-Aldrich (St. Louis, MO, U.S.A.). Compound C, LY294002 (cat. no. 11130), PD 98059 (cat. no. 4192), capsazepine (cat. no. 0464), and KC7F2 (cat. no. 4324) were obtained from Tocris (Cookson, Bristol, U.K.); fetal bovine serum (FBS, cat. no. 10082147),


https://doi.org/10.1021/acsomega.4c03539
ACS Omega 2024, 9, 29829−29839

and trypsin (cat. no. 15400054) were purchased from Gibco-BRL (Grand Island, NY, U.S.A.). Lipofectamine RNAimax reagent (cat. no. 13778150) and MitoSOX Mitochondrial Superoxide Indicators, for live-cell imaging (cat. no. M36008) were acquired from Thermo Fisher Scientific (Waltham, MA, U.S.A.). Cell counting kit-8 (CCK-8; catalog no. GK10001) was provided by Glpbio technology (Montclair, CA, U.S.A.). Primary antibodies for phospho-AKT (Ser473; p-AKT, catalog no. 4060), AKT (cat. no. 9272), phospho-ERK Thr202/Tyr204 (p-ERK, catalog no. 4370), ERK (cat. no. 4695), and KLF4 (cat. no. 4038) were obtained from Cell Signaling Technology (Beverly, MA, U.S.A.). Antibodies against PCNA (Cat. #sc-56), cyclin D1 (cat. no. sc-8396), cyclin E1 (cat. no. sc-377100), HIF-1$\alpha$ (cat. no. sc-53546), TRPV1 (cat. no. sc-398417), MMP2 (cat. no. sc-13595), MMP9 (catalog no. sc393859), transgelin (SM22; cat. no. sc-53932), and $\beta$-actin (cat. no. sc-47778) were sourced from Santa Cruz Biotechnology (Dallas, TX, U.S.A.). All other chemicals used were of the highest commercial grade available.

**4.3. Culture and Treatment.** The rat vascular smooth muscle cell line (RVSMC) was obtained from Cell Applications, Inc. (San Diego, CA, U.S.A.). Cells were cultured in DMEM (Welgene, Gyeongsan-si, Gyeongsangbuk-do, Korea) containing 10% FBS and 1% (v/v) penicillin/streptomycin at 37 °C in a humidified incubator with 5% $CO_2$. All experiments were conducted with cells between passages 5 and 11. High glucose (HG; 25 mM) was used as a model to investigate the role of citropten in VSMCs migration and proliferation as described in ref 23. Citropten was diluted in DMSO and applied for the experiment as described in the figure legends, respectively.

**4.4. Cell Viability.** To determine the toxicity effect of citropten, a MTT assay was conducted. Briefly, RVMSCs were seeded in 96-well plates at a density of $1 \times 10^4$ cells per well. Following that, the cells were pretreated with various concentrations of citropten and then treated with HG for an additional 48 h. In the MTT assay, the medium was discarded and cells were incubated with MTT solution (final concentration, 0.5 mg/mL) for 30 min. The formed formazan crystals were solubilized with DMSO and quantified by the absorbance at 550 nm.

**4.5. Cell Proliferation Assay.** CCK-8 kit was used to detect the effect of citropten on the proliferation of RVSMCs according to the manufacturer's protocol. Briefly, RVSMCs seeded in 96-well plates at a density of $1 \times 10^4$ cells/well. Upon adherence to the plates, cells were starved with serum-free DMEM overnight. Next, they were treated with different concentrations of citropten (10, 20, and 40 $\mu$M) and incubated for 48 h. CCK solution was directly added to each well (20 $\mu$L/well), and cells were incubated for 1−4 h in the incubator; the optical density (OD) at 450 nm was measured for each well using an automatic microplate reader.

**4.6. Transwell Migration Assay.** A transwell chamber was used to detect the migratory ability of RVSMCs. Briefly, RVSMC were seeded into the upper chamber at a density of $1 \times 10^5$ cells/well with serum-free DMEM. The lower chambers were filled with 800 $\mu$L DMEM with 20% FBS. On next day, cells were exposed with different concentrations of citropten (10, 20, and 40 $\mu$M) in absence or presence of HG. After incubation for 48 h, the lower side was fixed with 4% paraformaldehyde. After 20 min, the migrated cells were stained with 0.1% crystal violet staining solution for 15 min. The migrated cells were randomly captured using an inverted fluorescence microscope (Olympus U-CMAD3, Tokyo, Japan). The average number of cells that migrated was assayed by using ImageJ software.

**4.7. Wound Healing Assay.** Briefly, RVSMCs were treated with different concentrations of citropten (10, 20, and 40 $\mu$M) for 24 h in DMEM in the absence or presence of HG. Then, a horizontal wound was scratched with a sterile 10 $\mu$L pipet tip, and suspended cells were washed away with PBS twice. Images of each well were captured at 0 and 48 h. Wound closure was estimated based on the widths of the wounds at 0 and 48 h with a microscope using ImageJ v1.42l analysis software. Wound closures were calculated via the equation below: ((0 h) area − (48 h) area)/(0 h) area.

**4.8. Western Blotting.** Protein samples were extracted by using RIPA lysis buffer (25 mM Tris-HCl pH 7.6, 150 mM NaCl, 1% NP-40, 1% sodium deoxycholate, and 0.1% SDS). The protein concentrations were determined using a protein assay kit (Bradford Reagent, Sigma-Aldrich, St. Louis, MO, U.S.A.). Aliquots of the lysates were boiled for 5 min and electrophoresed in SDS-PAGE gels. Next, the proteins were transferred to PVDF membranes. After being blocked with 5% skim milk, the blots were incubated with the primary antibodies (at 1:500−1:1000) at 4 °C overnight. Next, the membranes were incubated with the secondary antimouse or -rabbit antibody (at 1:1000−1:2000). Finally, the membranes were exposed to the Detection Reagent Luminol Enhancer Solution (Thermo Scientific, Rockford, U.S.A.). Blots bands were quantified by densitometry using the ImageJ program.

**4.9. Realtime-PCR.** Total RNA from cell culture was extracted from cultured VSMCs using TRI Reagent Solution (Invitrogen, Massachusetts, USA) according to the manufacturer's instructions. The reverse transcription of the RNA was performed by using an RT PreMix kit (Enzynomics, Daejeon, Korea). Real-time PCR reactions were run on a CFX connect optics Module (Biorad, California, USA) instrument using BioFACT Real-time PCR Master mix was adopted following the sets: predegeneration for 10 min at 95 °C, and 45 cycles of 15 s at 95 °C and 60 s at 60 °C. The mRNA levels of the genes were normalized to *gapdh*. The gene expression was calculated using the following equation: gene expression = $2^{-\Delta\Delta CT}$, where $\Delta\Delta CT$ = (Ct *target* − Ct *gapdh*). The PCR primer sequences used in this study are listed in Supporting Information, Table 1.

**4.10. Reactive Oxygen Species (ROS) Assay.** The ROS levels in VSMCs were detected using DCFHDA as a probe to estimate the ROS of the cell. Briefly, RVSMC cells were incubated with DCFHDA (5 $\mu$M) at 37 °C for 30 min in the dark. The cells were then rinsed with PBS twice, and the fluorescence intensity was spectrofluorometer at an excitation and emission wavelength of 485 and 530 nm, respectively.

**4.11. Immunofluorescence Staining.** VSMCs were seeded on coverslips in 12-well plates for 24 h. After the designated incubation, the cells were fixed with 4% PFA for 20 min and permeabilized with 0.2% Triton X-100 for 10 min at RT. Next, the cells were blocked with 5% BSA for 1 h and incubated with the primary antibody against SM22 (1:200) at 4 °C overnight, followed by incubation with secondary antibody (1:1000; Goat antimouse Alexa Fluor 488, Cat. #A28175; Thermo fisher Scientific) in the dark for 4 h at RT. They were rinsed with PBS several times. The cells were mounted with ProLong Gold Antifade Mountant containing DAPI (Invitrogen, 168 Third Avenue, Waltham, MA, U.S.A.) and then viewed using an EVOS FL Cell Imaging System


https://doi.org/10.1021/acsomega.4c03539
ACS Omega 2024, 9, 29829−29839

(Thermo Fisher Scientific, 168 Third Avenue, Waltham, MA U.S.A.).

**4.12. Silencing RNA Transfection.** Cells were transfected with silencing RNA (siRNA): TRPV1 siRNA (sc-108093) and control siRNA (sc-37007) were purchased from Santa Cruz Biotechnology, Inc. siRNAs were transfected into VSMC cells using Lipofectamine RNAimax reagent (Thermo Fisher Scientific) When VSMCs reached approximately 70−80% confluence, a mixture of siRNA and Lipofectamine RNAimax reagent was added to the cells. The medium was replaced at 6 h post-transfection, and citropten was applied as indicated. Transfection efficacy was assessed by Western blotting.

**4.13. MitoSOX Red Mitochondrial Superoxide Staining.** The assumption that mitochondria serve as the major intracellular source of ROS has been largely based on experiments. Therefore, we detected superoxide in the mitochondria of live cells under HG stimulation using MitoSOX Red mitochondrial superoxide according to the manufacturer's instructions. Briefly, RVSMC cells were seed on 48-well plate at $3 \times 10^4$ cells/well and treatment as described in figures legend. Cells were stained with 5 $\mu$M MitoSOX reagent solution prepared in HBSS buffer for 30 min at 37 °C and protected from light. Then, cells were washed gently three times with warm buffer and visualized under microscopy.

**4.14. Molecular Docking.** The structure of TRPV1 was downloaded from the RSCB Protein Data Bank Web site with the PDB ID 7L2H. The protein was prepared for docking using BIOVIA Discovery Studio v21.1 (Dassault Systèmes, San Diego, CA, U.S.A.), and computational docking was predicted using AutoDockTools 1.5.6 and AutoDock Vina 1.1.2 29. The 3D structure of citropten was established using Spartan'18 (Wave function Inc., Irvine, CA, U.S.A.). The strongest molecular link was believed to be represented by the lowest number, based on the binding affinity score and the root-mean-square deviation (RMSD). The interaction between citropten and 7L2H was predicted, and BIOVIA Discovery Studio v21.1 was utilized to illustrate the graphic result. $\pi-\pi$ bonds, hydrogen bonds, van der Waals interactions, and the interaction distance between amino acids and the active sites of citropten were predicted.

**4.15. Statistical.** Three independent biological experiments were repeated, and the quantitative data are presented as the mean ± standard deviation. One-way ANOVA analysis of variance accompanied by Student−Newman−Keuls test were performed to compare the means. $P < 0.05$ was considered to indicate a statistically significant difference.

## ■ ASSOCIATED CONTENT

### Supporting Information

The Supporting Information is available free of charge at https://pubs.acs.org/doi/10.1021/acsomega.4c03539.

Primer sequences for real-time PCR analysis (Table S1); The effect of citropten with SM22 expression in RVSMCs under HG stimulation (Figure S1); The expression of TRPV1 after transfection with siRNA TRPV1 in RVSMCs (Figure S2) (PDF)

## ■ AUTHOR INFORMATION


### Corresponding Author

**Gil-Saeng Jeong** − *College of Pharmacy, Chungnam National University, Daejeon 34134, Republic of Korea;* orcid.org/0000-0002-1882-0256; Email: gsjeong@cnu.ac.kr

### Authors

**Thi Hoa Pham** − *College of Pharmacy, Chungnam National University, Daejeon 34134, Republic of Korea*

**Nguyen Minh Trang** − *College of Pharmacy, Chungnam National University, Daejeon 34134, Republic of Korea*

**Eun-Nam Kim** − *College of Pharmacy, Chungnam National University, Daejeon 34134, Republic of Korea*

**Hye Gwang Jeong** − *College of Pharmacy, Chungnam National University, Daejeon 34134, Republic of Korea;* orcid.org/0000-0002-8020-8914

Complete contact information is available at: https://pubs.acs.org/10.1021/acsomega.4c03539

### Author Contributions

‡T.H.P. and N.M.T. equally contributed to this work.


### Author Contributions

T.H.P.: Conceptualization, Methodology, Investigation, Data curation, Writing−original draft. N.M.T.: Conceptualization, Methodology, Investigation, Data curation, Writing−review and editing. E.-N.K.: Methodology, Data curation. H.G.J.: Conceptualization. G.-S.J.: Project administration, Conceptualization, Supervision, Writing−review and editing.

### Notes

The authors declare no competing financial interest.

## ■ ACKNOWLEDGMENTS

This research was conducted with support from National Research Foundation grants (2022R1A5A7085156).

## ■ ABBREVIATIONS

CCK-8, cell counting kit-8; CPZ, capsazepine; EGCG, Epigallocatechin gallate; HG, high glucose; HIF-1$\alpha$, hypoxia-inducible factor-1$\alpha$; KLF4, Krüppel-like factor 4; MMP, matrix metalloproteinases; NAC, N-acetyl-L-cysteine; PCNA, proliferating cell nuclear antigen; ROS, reactive oxygen species; RVSMCs, rat vascular smooth muscle cells; SM22, transgelin; TRPV1, transient receptor potential vanilloid 1.

## ■ REFERENCES


(1) Timmis, A.; Townsend, N.; Gale, C. P.; Torbica, A.; Lettino, M.; Petersen, S. E.; Mossialos, E. A.; Maggioni, A. P.; Kazakiewicz, D.; May, H. T.; De Smedt, D.; Flather, M.; Zuhlke, L.; Beltrame, J. F.; Huculeci, R.; Tavazzi, L.; Hindricks, G.; Bax, J.; Casadei, B.; Achenbach, S.; Wright, L.; Vardas, P. European society of cardiology: cardiovascular disease statistics 2019 (Executive Summary). *Eur. Heart J.* **2020**, *6*, 7−9.

(2) Townsend, N.; Kazakiewicz, D.; Lucy Wright, F.; Timmis, A.; Huculeci, R.; Torbica, A.; Gale, C. P.; Achenbach, S.; Weidinger, F.; Vardas, P. Epidemiology of cardiovascular disease in Europe. *Nat. Rev. Cardiol.* **2022**, *19*, 133−143.

(3) Ashino, T.; Yamamoto, M.; Numazawa, S. Nrf2/Keap1 system regulates vascular smooth muscle cell apoptosis for vascular homeostasis: role in neointimal formation after vascular injury. *Sci. Rep.* **2016**, *6*, 26291.

(4) Cao, G.; Xuan, X.; Hu, J.; Zhang, R.; Jin, H.; Dong, H. How vascular smooth muscle cell phenotype switching contributes to vascular disease. *Cell Commun. Signal.* **2022**, *20*, 180.

(5) Shi, J.; Yang, Y.; Cheng, A.; Xu, G.; He, F. Metabolism of vascular smooth muscle cells in vascular diseases. *Am. J. Physiol. Heart Circ. Physiol.* **2020**, *319*, H613−H631.

(6) Hayashi, K. i.; Takahashi, M.; Nishida, W.; Yoshida, K.; Ohkawa, Y.; Kitabatake, A.; Aoki, J.; Arai, H.; Sobue, K. Phenotypic modulation of vascular smooth muscle cells induced by unsaturated lysophosphatidic acids. *Circ. Res.* **2001**, *89*, 251−258.

(7) Louis, S. F.; Zahradka, P. Vascular smooth muscle cell motility: From migration to invasion. *Exp. Clin. Cardiol.* **2010**, *15* (4), e75−e85.
(8) Petsophonsakul, P.; Furmanik, M.; Forsythe, R.; Dweck, M.; Schurink, G. W.; Natour, E.; Reutelingsperger, C.; Jacobs, M.; Mees, B.; Schurgers, L. Role of vascular smooth muscle cell phenotypic switching and calcification in aortic aneurysm formation. *Arterioscler Thromb Vasc Biol.* **2019**, *39*, 1351−1368.
(9) Chakraborty, R.; Chatterjee, P.; Dave, J. M.; Ostriker, A. C.; Greif, D. M.; Rzucidlo, E. M.; Martin, K. A. Targeting smooth muscle cell phenotypic switching in vascular disease. *VS-Vasc. Sci.* **2021**, *2*, 79−94.
(10) Lu, Q. B.; Wan, M. Y.; Wang, P. Y.; Zhang, C. X.; Xu, D. Y.; Liao, X.; Sun, H. J. Chicoric acid prevents PDGF-BB-induced VSMC dedifferentiation, proliferation and migration by suppressing ROS/NFκB/mTOR/P70S6K signaling cascade. *Redox Biol.* **2018**, *14*, 656−668.
(11) Stein, J. J.; Iwuchukwu, C.; Maier, K. G.; Gahtan, V. Thrombospondin-1-induced vascular smooth muscle cell migration and proliferation are functionally dependent on microRNA-21. *Surgery* **2014**, *155*, 228−33.
(12) Li, P.; Zhu, N.; Yi, B.; Wang, N.; Chen, M.; You, X.; Zhao, X.; Solomides, C. C.; Qin, Y.; Sun, J. MicroRNA-663 regulates human vascular smooth muscle cell phenotypic switch and vascular neointimal formation. *Circ. Res.* **2013**, *113*, 1117−27.
(13) Tóth, A.; Czikora, A.; Pásztor, E. T.; Dienes, B.; Bai, P.; Csernoch, L.; Rutkai, I.; Csató, V.; Mányiné, I. S.; Pórszász, R.; Edes, I.; Papp, Z.; Boczán, J. Vanilloid receptor-1 (TRPV1) expression and function in the vasculature of the rat. *J. Histochem. Cytochem.* **2014**, *62*, 129−44.
(14) Zhang, F.; Jara-Oseguera, A.; Chang, T.-H.; Bae, C.; Hanson, S. M.; Swartz, K. J. Heat activation is intrinsic to the pore domain of TRPV1. *Proc. Natl. Acad. Sci. U. S. A.* **2018**, *115* (2), E317−E324.
(15) Baylie, R. L.; Brayden, J. E. TRPV channels and vascular function. *Acta physiologica* **2011**, *203*, 99−116.
(16) Ma, L.; Zhong, J.; Zhao, Z.; Luo, Z.; Ma, S.; Sun, J.; He, H.; Zhu, T.; Liu, D.; Zhu, Z.; Tepel, M. Activation of TRPV1 reduces vascular lipid accumulation and attenuates atherosclerosis. *Cardiovasc. Res.* **2011**, *92*, 504−13.
(17) Phan, T. X.; Ton, H. T.; Gulyás, H.; Pórszász, R.; Tóth, A.; Russo, R.; Kay, M. W.; Sahibzada, N.; Ahern, G. P. TRPV1 expressed throughout the arterial circulation regulates vasoconstriction and blood pressure. *J. Physiol.* **2020**, *598*, 5639−5659.
(18) Wang, S.; Jia, C. TRPV1 inhibits smooth muscle cell phenotype switching in a mouse model of abdominal aortic aneurysm. *Channels* **2020**, *14*, 59−68.
(19) Zhou, Y.; Wang, X.; Guo, L.; Chen, L.; Zhang, M.; Chen, X.; Li, J.; Zhang, L. TRPV1 activation inhibits phenotypic switching and oxidative stress in vascular smooth muscle cells by upregulating PPARα. *Biochem. Biophys. Res. Commun.* **2021**, *545*, 157−163.
(20) Alesiani, D.; Cicconi, R.; Mattei, M.; Montesano, C.; Bei, R.; Canini, A. Cell cycle arrest and differentiation induction by 5,7-dimethoxycoumarin in melanoma cell lines. *Int. J. Oncol.* **2008**, *32* (2), 425−34.
(21) Yang, W.; Wang, H. 5,7-Dimethoxycoumarin prevents chronic mild stress induced depression in rats through increase in the expression of heat shock protein-70 and inhibition of monoamine oxidase-A levels. *Saudi J. Biol. Sci.* **2018**, *25*, 253−258.
(22) Trang, N. M.; Kim, E. N.; Pham, T. H.; Jeong, G. S. Citropten ameliorates osteoclastogenesis related to MAPK and PLCγ/Ca(2+) signaling pathways through the regulation of amyloid beta. *J. Agric. Food Chem.* **2023**, *71*, 10037−10049.
(23) Zhang, W.; Chen, S.; Zhang, Z.; Wang, C.; Liu, C. FAM3B mediates high glucose-induced vascular smooth muscle cell proliferation and migration via inhibition of miR-322-5p. *Sci. Rep.* **2017**, *7*, 2298.
(24) Sun, Y.; Liu, W.-Z.; Liu, T.; Feng, X.; Yang, N.; Zhou, H.-F. Signaling pathway of MAPK/ERK in cell proliferation, differentiation, migration, senescence and apoptosis. *J. Recept. Signal Transduct.* **2015**, *35*, 600−604.
(25) Wei, L.; Zhou, Q.; Tian, H.; Su, Y.; Fu, G. H.; Sun, T. Integrin β3 promotes cardiomyocyte proliferation and attenuates hypoxia-induced apoptosis via regulating the PTEN/Akt/mTOR and ERK1/2 pathways. *Int. J. Biol. Sci.* **2020**, *16*, 644−654.
(26) Han, X.-J.; Zhang, W.-F.; Wang, Q.; Li, M.; Zhang, C.-B.; Yang, Z.-J.; Tan, R.-J.; Gan, L.-J.; Zhang, L.-L.; Lan, X.-M.; Zhang, F.-L.; Hong, T.; Jiang, L.-P. HIF-1α promotes the proliferation and migration of pulmonary arterial smooth muscle cells via activation of Cx43. *J. Cell Mol. Med.* **2021**, *25*, 10663−10673.
(27) Zhang, H.; Nan, W.; Song, X.; Wang, S.; Si, H.; Li, G. Knockdown of HIF-1α inhibits the proliferation and migration of outer root sheath cells exposed to hypoxia in vitro: An involvement of Shh pathway. *Life Sci.* **2017**, *191*, 82−89.
(28) Chen, S.; Zhang, M.; Xing, L.; Wang, Y.; Xiao, Y.; Wu, Y. HIF-1α Contributes to proliferation and invasiveness of neuroblastoma cells via SHH Signaling. *PLoS One* **2015**, *10*, No. e0121115.
(29) Guo, B. C.; Wei, J.; Su, K. H.; Chiang, A. N.; Zhao, J. F.; Chen, H. Y.; Shyue, S. K.; Lee, T. S. Transient receptor potential vanilloid type 1 is vital for (−)-epigallocatechin-3-gallate mediated activation of endothelial nitric oxide synthase. *Mol. Nutr Food Res.* **2015**, *59*, 646−57.
(30) Shim, S. Y.; Lee, G. B.; Shim, J. S.; Jung, S. J.; Kim, H. C. Association between a family history of diabetes and carotid artery atherosclerosis in Korean adults. *Epidemiol Health* **2021**, *43*, e2021049.
(31) Coutinho, M.; Gerstein, H. C.; Wang, Y.; Yusuf, S. The relationship between glucose and incident cardiovascular events. A metaregression analysis of published data from 20 studies of 95,783 individuals followed for 12.4 years. *Diabetes care* **1999**, *22*, 233−40.
(32) Joseph, J. J.; Deedwania, P.; Acharya, T.; Aguilar, D.; Bhatt, D. L.; Chyun, D. A.; Di Palo, K. E.; Golden, S. H.; Sperling, L. S. Comprehensive management of cardiovascular risk factors for adults with type 2 diabetes: a scientific statement from the American Heart Association. *Circulation* **2022**, *145*, e722−e759.
(33) Lin, Y. C.; Chen, L. H.; Varadharajan, T.; Tsai, M. J.; Chia, Y. C.; Yuan, T. C.; Sung, P. J.; Weng, C. F. Resveratrol inhibits glucose-induced migration of vascular smooth muscle cells mediated by focal adhesion kinase. *Mol. Nutr. Food Res.* **2014**, *58*, 1389−401.
(34) Wu, Y. T.; Chen, L.; Tan, Z. B.; Fan, H. J.; Xie, L. P.; Zhang, W. T.; Chen, H. M.; Li, J.; Liu, B.; Zhou, Y. C. Luteolin inhibits vascular smooth muscle cell proliferation and migration by inhibiting TGFBR1 signaling. *Front. Pharmacol.* **2018**, *9*, 1059.
(35) Han, D. W.; Lee, M. H.; Kwon, B. J.; Kim, H. L.; Hyon, S. H.; Park, J. C. Selective inhibitory effect of epigallocatechin-3-gallate on migration of vascular smooth muscle cells. *Molecules* **2010**, *15*, 8488−500.
(36) Chen, K.; Li, Y.; Zhang, X.; Ullah, R.; Tong, J.; Shen, Y. The role of the PI3K/AKT signalling pathway in the corneal epithelium: recent updates. *Cell Death Dis.* **2022**, *13*, 513.
(37) Xu, J.; Liu, X.; Zhao, F.; Zhang, Y.; Wang, Z. HIF1α overexpression enhances diabetic wound closure in high glucose and low oxygen conditions by promoting adipose-derived stem cell paracrine function and survival. *Stem Cell Res. Ther.* **2020**, *11*, 148.
(38) Isoe, T.; Makino, Y.; Mizumoto, K.; Sakagami, H.; Fujita, Y.; Honjo, J.; Takiyama, Y.; Itoh, H.; Haneda, M. High glucose activates HIF-1-mediated signal transduction in glomerular mesangial cells through a carbohydrate response element binding protein. *Kidney Int.* **2010**, *78*, 48−59.
(39) Chen, Q.; Wang, Q.; Zhu, J.; Xiao, Q.; Zhang, L. Reactive oxygen species: key regulators in vascular health and diseases. *Br. J. Pharmacol.* **2018**, *175*, 1279−1292.
(40) Bujak, J. K.; Kosmala, D.; Szopa, I. M.; Majchrzak, K.; Bednarczyk, P. Inflammation, cancer and immunity-implication of TRPV1 channel. *Front Oncol.* **2019**, *9*, 1087.
(41) Zhang, C.; Ye, L.; Zhang, Q.; Wu, F.; Wang, L. The role of TRPV1 channels in atherosclerosis. *Channels* **2020**, *14*, 141−150.


https://doi.org/10.1021/acsomega.4c03539
*ACS Omega* 2024, 9, 29829−29839

(42) Hao, X.; Chen, J.; Luo, Z.; He, H.; Yu, H.; Ma, L.; Ma, S.; Zhu, T.; Liu, D.; Zhu, Z. TRPV1 activation prevents high-salt diet-induced nocturnal hypertension in mice. *Pflügers Archiv* **2011**, *461*, 345−53.



https://doi.org/10.1021/acsomega.4c03539
*ACS Omega* 2024, 9, 29829−29839